DOI: 10.1002/ange.201207628

Computational Photochemistry

Photoinduced Ultrafast Wolff Rearrangement: A Non-Adiabatic Dynamics Perspective**

*Ganglong Cui and Walter Thiel**

α-Diazocarbonyl compounds play an important role in organic synthesis, photolithography, drug delivery, and industrial chemistry.[1–4] Upon irradiation they can undergo a Wolff rearrangement, with loss of nitrogen and ketene formation (Figure 1). This rearrangement was discovered more than a century ago, but its detailed reaction mechanism remains elusive.[1–8]

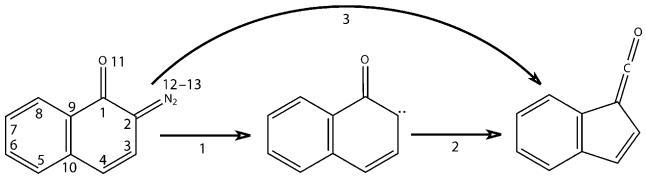

Figure 1. Wolff rearrangement of 2-diazo-1-naphthoquinone (DNQ): stepwise (1–2) and concerted (3) mechanisms. The numbering scheme for the atoms is shown for the DNQ reactant.

Experimentally, both concerted and stepwise mechanisms have been proposed.[1–12] On the theoretical side, previous electronic structure calculations[13,14] have focused on diazo compounds that do not undergo the Wolff rearrangement. Recently, Blancafort and co-workers[15,16] simulated the photochemical Wolff rearrangement in 2-diazo-1-naphthoquinone (DNQ) using high-level electronic structure calculations and quantum dynamics based on a fitted three-dimensional two-state model surface. An extended S_1/S_0 conical intersection seam was found to play a crucial role in regulating the reaction. Ketene and carbene formation was observed within the first 100 fs of their quantum dynamics. One limitation of these quantum dynamics simulations on a three-dimensional model surface is that they ignore the influence from the other degrees of freedom, assuming that the three selected coordinates are sufficient to describe the reaction properly; in addition, the initial S_2 relaxation dynamics has not been considered explicitly.[15,16] Given this situation, it is desirable to perform full-dimensional quantum-classical non-adiabatic dynamics starting from the initially populated bright S_2 state to gain further complementary insight into the mechanism. Quantum-classical dynamics simulations have recently been applied successfully to elucidate photoinduced conversion processes in various molecules and environments.[17–28] These studies have mostly focused on ultrafast photophysical processes, rather than on photochemical reactions that may branch into several chemically distinct product channels.

Herein, we report full-dimensional non-adiabatic and adiabatic dynamics simulations of the ultrafast Wolff rearrangement in DNQ.[29,30] The chosen computational methods and their validation are described in the Supporting Information. Trajectory surface hopping (TSH) calculations were carried out using the OM2/MRCI method to calculate the required energies and gradients "on the fly". Out of 200 trajectories 158 were run successfully and used for analysis.[31]

The deactivation of the S_2 state in DNQ is ultrafast. In all 158 trajectories, the system decays to the S_0 state within approximately 200 fs (Figure S7 in the Supporting Information). The S_1 population quickly builds up, reaches a maximum of 0.3 after 50 fs, and approaches zero after less than 200 fs. In contrast, the S_2 state population decreases monotonically and the S_0 state population increases monotonically. Fitting with a three-state model[21] yields two excited-state lifetimes: 70 fs for the S_2 state and 33 fs for the S_1 state (see Supporting Information for details). Assuming that the $S_2 \rightarrow S_1$ and $S_1 \rightarrow S_0$ conversions occur sequentially, we arrive at an overall internal conversion time from S_2 to S_0 of approximately 100 fs. These excited-state lifetimes are consistent with the experimental evidence.[29] Brixner and co-workers observed that the ketene intermediate appears within 300 fs (the time resolution of the experiment) in their femtosecond mid-infrared study of DNQ, and hence they proposed that the ketene is formed in a very fast concerted process involving N_2 loss and rearrangement. Furthermore, our computed S_1 excited-state lifetime (33 fs) is also close to the recent quantum dynamics estimate (20–40 fs).[15]

The top panel of Figure 2 shows the S_2/S_1 and S_1/S_0 conical intersection surfaces obtained from OM2/MRCI conical intersection optimizations with geometric constraints on both the C2–N12 distance and the C3-C2-N12-N13 dihedral angle. At the optimized constrained geometries, the energy gap between the two states is zero; the color code in Figure 2 indicates the energy relative to the corresponding minimum-energy conical intersection. In the S_2/S_1 case (Figure 2, top left), there is a clear local minimum region (between 1.4–1.5 Å and 80–100°) which is centered around the unconstrained S_2/S_1 minimum-energy conical intersection S2S1-MIN. In contrast, in the S_1/S_0 case, most of conical intersection surface is energetically rather shallow (except for short C2–N12 distances of less than 1.5 Å and nearly perpendicular C3-

[*] Dr. G. Cui, Prof. Dr. W. Thiel
Max-Planck-Institut für Kohlenforschung
Kaiser-Wilhelm-Platz 1, 45470 Mülheim an der Ruhr (Germany)
E-mail: thiel@mpi-muelheim.mpg.de

[**] G.L. is grateful for financial support from the Alexander von Humboldt Foundation.

Supporting information for this article is available on the WWW under http://dx.doi.org/10.1002/anie.201207628.

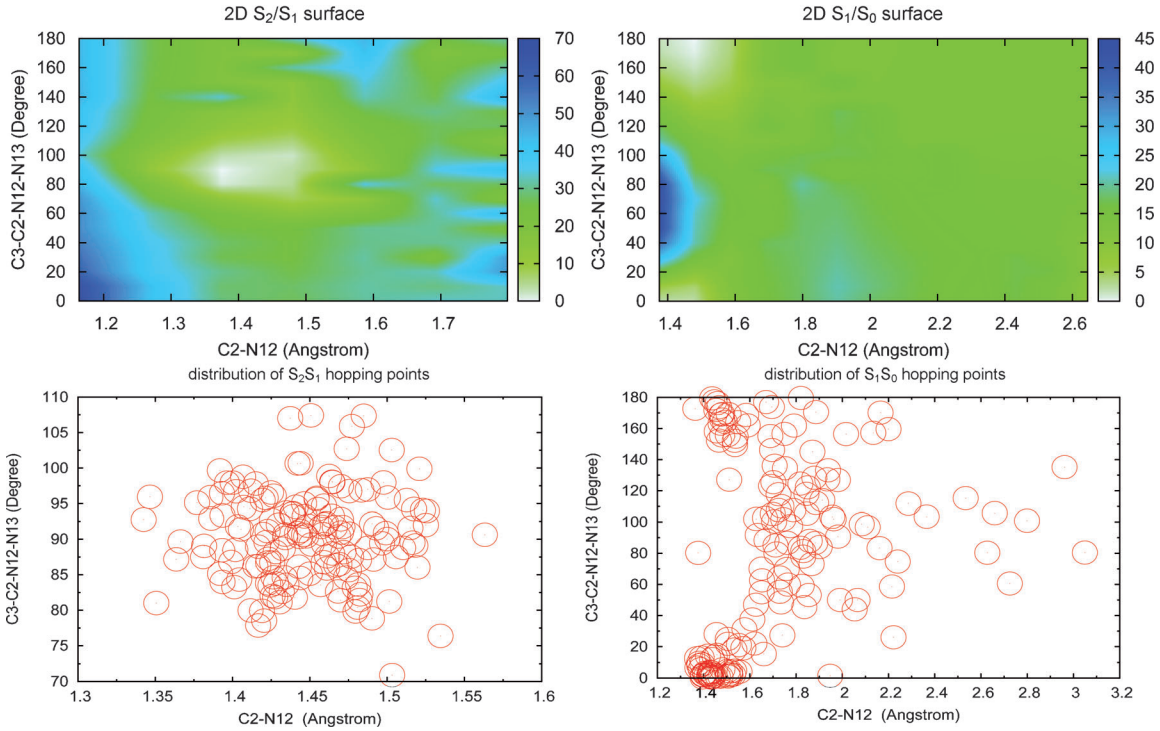

Figure 2. Top: two-dimensional S_2/S_1 and S_1/S_0 conical intersection surfaces with geometric constraints on the C2–N12 distance and the C3-C2-N12-N13 dihedral angle (energies in kcal mol^{-1} relative to the minimum-energy conical intersection). Bottom: $S_2 \rightarrow S_1$ and $S_1 \rightarrow S_0$ hopping-point distributions in 158 trajectories.

C2-N12-N13 torsions of 70–110°) indicating that most of this flat region can be easily accessed by trajectories. The topological characteristics of these surfaces are reflected in the OM2/MRCI non-adiabatic dynamics simulations (see bottom panel of Figure 2). The $S_1 \rightarrow S_0$ hopping points are widely distributed over the S_1/S_0 conical intersection surface, whereas the $S_2 \rightarrow S_1$ hopping points tend to cluster around the minimum of the S_2/S_1 conical intersection surface, that is, S2S1-MIN. The C3-C2-N12-N13 torsion is clearly important for the $S_1 \rightarrow S_0$ internal conversion in DNQ, because only a little energy is needed to maintain the S_1/S_0 degeneracy during such twisting motion (resulting in an extended conical intersection region). To achieve a realistic mechanistic scenario, it is thus essential to include this coordinate in dynamics treatments that employ reduced model surfaces.[15]

The product distribution at the end of the 1 ps TSH simulations is indicated in Figure 3. The ketene product of the concerted Wolff rearrangement is found in seven out of 158 trajectories; 39 trajectories return to the ground-state starting point, and the remaining 112 trajectories are roaming the carbene region (see Figure 3). Our computed carbene:ketene ratio (16:1) is higher than that predicted by Blancafort et al. (4:1) in their 100 fs quantum dynamics.[15] The ketene quantum yield in the current simulations is still very low after 1 ps (ca. 5 %), but it is expected to increase with time through the conversion of the "hot" carbene intermediate into the ketene (stepwise Wolff rearrangement). We have simulated this ground-state process by performing 10 ps Born–Oppenheimer molecular dynamics (BOMD) for the carbene, using the final positions and velocities of the carbene fragment in

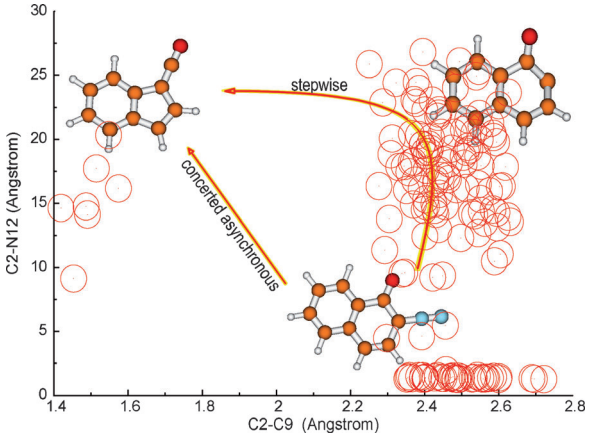

Figure 3. Product distribution of the 158 trajectories at the end of the 1 ps non-adiabatic simulations. Red circles indicate the final geometries after 1 ps (C orange, O red, N blue).

the TSH trajectories as initial conditions in each of the 112 runs (see Supporting Information for technical details). In these BOMD simulations, 36 of the 112 trajectories evolve from the "hot" carbene to the ketene region, thus increasing the overall ketene quantum yield to around 27 % after 10 ps (Figure S13). The OM2/MRCI barrier for the ground-state carbene–ketene rearrangement is 7.0 kcal mol^{-1} (Figure S11), close to the CASPT2 value of 7.8 kcal mol^{-1}.[15]

We thus observe both concerted asynchronous and stepwise Wolff rearrangements in our full-dimensional dynamics simulations. In one of the rare examples for the

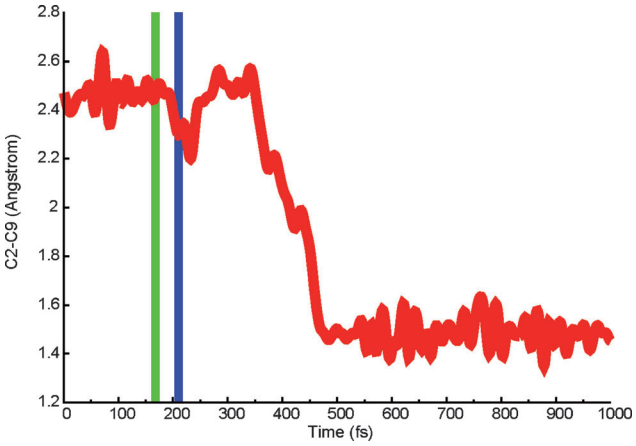

Figure 4. One typical trajectory for the concerted asynchronous Wolff rearrangement. The $S_2 \rightarrow S_1$ hop is marked in green at 167 fs, and the $S_1 \rightarrow S_0$ hop in blue at 210 fs.

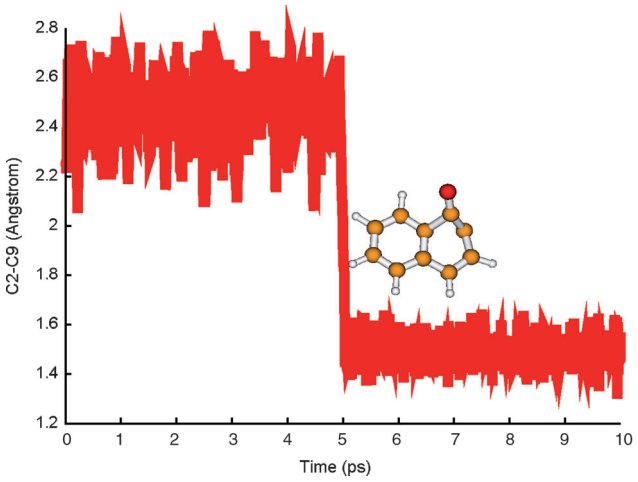

Figure 5. One typical trajectory for the second phase of the stepwise Wolff rearrangement (carbene-to-ketene rearrangement).

concerted asynchronous Wolff rearrangement (Figure 4), the molecule is excited to the bright S_2 ($\pi\pi^*$) state and undergoes an $S_2 \rightarrow S_1$ internal conversion after 167 fs, which triggers an immediate elongation of the C2–N12 bond that takes the molecule to the extended S_1/S_0 conical intersection seam (Figure 2). This leads to an ultrafast $S_1 \rightarrow S_0$ decay (after 43 fs in this trajectory, compared with 20–40 fs in the quantum dynamics work[15]). In the S_0 state, the C2···N12 distance then continues to increase until the end of the 1 ps dynamics run, while the C2···C9 distance starts to decrease after about 100 fs to form a covalent C2–C9 bond. This effectively concerted process is finished after approximately 400 fs, in reasonable agreement with the experimental finding that irradiation of a DNQ derivative in methanol yields the ketene product within 300 fs.[29]

The trajectories that produce the carbene intermediate start out in a similar manner (for an example, see the middle panel of Figure S9). After the initial $S_2 \rightarrow S_1$ internal conversion, the C2–N12 bond lengthens and then breaks after the ultrafast $S_1 \rightarrow S_0$ decay, with release of a nitrogen molecule. Until the end of the 1 ps simulation, the C2–C9 distance then just fluctuates around its equilibrium value of 2.4 Å, thus retaining a carbene structure. In our 1 ps TSH simulations, more than half of the trajectories end up at such carbene intermediates, many of which rearrange within 10 ps to the more stable ketene product (stepwise Wolff rearrangement) according to the BOMD simulations (Figure S13). Figure 5 shows the second phase of a typical stepwise rearrangement, where the ring contraction happens after 5 ps. The present dynamics study thus suggests that both the concerted and the stepwise pathway are feasible in the photochemistry of DNQ.

In our simulations, 25% of the trajectories return to ground-state DNQ within 1 ps, without undergoing any chemical reaction; 27% of the dynamics runs end up at the ketene after 10 ps, and 48% at the carbene. Experimentally, there is evidence for a carbene intermediate, but the photo-induced fragmentation processes in solution are reported to be complete after 8 ps,[10] indicating that our gas-phase simulations overestimate the lifetime of the carbene intermediate in solution (ca. 29 ps according to Figure S13). On the other hand, our computed gas-phase quantum yield of ketene (27% after 10 ps) compares reasonably well with the measured values of 54% for DNQ in methanol[10] and of 32% for a sulfonated DNQ derivative in both methanol and water.[29] We also note in this context that solvent effects may influence the carbene:ketene ratio because surrounding solvent molecules may affect the relative ease of nitrogen release on the concerted and stepwise pathways. The simulation of such solvent effects is beyond the scope of the present work.

In summary, we have explored the photochemical Wolff rearrangement of DNQ by performing full-dimensional non-adiabatic dynamics simulations starting from the initially populated bright S_2 state, as well as ground-state BOMD simulations starting from the "hot" carbene intermediate. The present work demonstrates that trajectory surface-hopping dynamics can well be applied to study the photochemistry of medium-size molecules with an extended conical intersection seam. The relevant coordinates for describing the photo-induced processes in DNQ include not only the C2–C9 and C2–N12 distances, but also the C3-C2-N12-N13 dihedral angle for out-of-plane motion. The TSH simulations branch into different channels at the extended S_1/S_0 conical intersection seam: the trajectories either return to the ground state of DNQ (ultrafast deactivation) or directly enter the ground-state ketene region (concerted reaction) or lead to a ground-state carbene intermediate that can then rearrange to the ketene (stepwise reaction). Mechanistically, we thus find that both the concerted asynchronous and stepwise mechanisms are accessible in the photochemical Wolff rearrangement, as has also been suggested for other diazocarbonyl compounds.[4–6] The detailed mechanistic scenario emerging from the simulations is consistent with recent time-resolved femtosecond experiments that show direct ketene formation within 300 fs[29] and with previous theoretical and experimental evidence that the ketene may also be formed by a stepwise mechanism via a carbene intermediate.[10,15,29] Methodologically, this work demonstrates that surface hopping dynamics is

capable of simulating not only photophysical processes, but also complicated photochemical reactions with several competing channels in medium-size organic molecules.[32]

Received: September 20, 2012
Revised: November 1, 2012
Published online: December 5, 2012

Keywords: diazocarbonyl compounds · excited states · non-adiabatic dynamics · surface hopping · Wolff rearrangement

[1] L. Wolff, *Justus Liebigs Ann. Chem.* **1902**, *325*, 129.
[2] H. Meier, K. P. Zeller, *Angew. Chem.* **1975**, *87*, 52; *Angew. Chem. Int. Ed. Engl.* **1975**, *14*, 32.
[3] W. Kirmse, *Eur. J. Org. Chem.* **2002**, 2193.
[4] G. Burdzinski, M. S. Platz, *J. Phys. Org. Chem.* **2010**, *23*, 308.
[5] G. T. Burdzinski, J. Wang, T. L. Gustafson, M. S. Platz, *J. Am. Chem. Soc.* **2008**, *130*, 3746.
[6] P. Rudolf, J. Buback, J. Aulbach, P. Nuernberger, T. Brixner, *J. Am. Chem. Soc.* **2010**, *132*, 15213.
[7] T. T. Tidwell, *Angew. Chem.* **2005**, *117*, 5926; *Angew. Chem. Int. Ed.* **2005**, *44*, 5778.
[8] K. P. Zeller, A. Blocher, P. Haiss, *Mini-Rev. Org. Chem.* **2004**, *1*, 291.
[9] M. Barra, T. A. Fisher, G. J. Gernigliaro, R. Sinta, J. C. Scaiano, *J. Am. Chem. Soc.* **1992**, *114*, 2630.
[10] J. J. M. Vleggaar, A. H. Huizer, P. A. Kraakman, W. P. M. Nijssen, R. J. Visser, C. A. G. O. Varma, *J. Am. Chem. Soc.* **1994**, *116*, 11754.
[11] K. Tanigaki, T. W. Ebbesen, *J. Am. Chem. Soc.* **1987**, *109*, 5883.
[12] K. Tanigaki, T. W. Ebbesen, *J. Phys. Chem.* **1989**, *93*, 4531.
[13] N. Yamamoto, F. Bernardi, A. Bottoni, M. Olivucci, M. A. Robb, S. Wilsey, *J. Am. Chem. Soc.* **1993**, *115*, 10605.
[14] J. F. Arenas, I. Lopez-Tocon, J. C. Otero, J. Soto, *J. Am. Chem. Soc.* **2002**, *124*, 1728.
[15] Q. S. Li, A. Migani, L. Blancafort, *J. Phys. Chem. Lett.* **2012**, *3*, 1056.
[16] Q. S. Li, A. Migani, L. Blancafort, *J. Phys. Chem. A* **2009**, *113*, 9413.
[17] M. Barbatti, H. Lischka, *J. Am. Chem. Soc.* **2008**, *130*, 6831.
[18] M. Boggio-Pasqua, M. A. Robb, G. Groenhof, *J. Am. Chem. Soc.* **2009**, *131*, 13580.
[19] M. Frutos, T. Andruniow, F. Santoro, N. Ferre, M. Olivucci, *Proc. Natl. Acad. Sci. USA* **2007**, *104*, 7764.
[20] M. Böckmann, N. L. Doltsinis, D. Marx, *Angew. Chem.* **2010**, *122*, 3454; *Angew. Chem. Int. Ed.* **2010**, *49*, 3382.
[21] E. Fabiano, W. Thiel, *J. Phys. Chem. A* **2008**, *112*, 6859.
[22] I. Tavernelli, E. Tapavicza, U. Rothlisberger, *J. Chem. Phys.* **2009**, *130*, 124107.
[23] R. Mitric, U. Werner, V. Bonacic-Koutecky, *J. Chem. Phys.* **2008**, *129*, 164118.
[24] O. Weingart, P. Altoe, M. Stenta, A. Bottoni, G. Orlandi, M. Garavelli, *Phys. Chem. Chem. Phys.* **2011**, *13*, 3645.
[25] T. Cusati, G. Granucci, M. Persico, *J. Am. Chem. Soc.* **2011**, *133*, 5109.
[26] S. Olsen, K. Lamothe, T. J. Martinez, *J. Am. Chem. Soc.* **2010**, *132*, 1192.
[27] Y. Lu, Z. Lan, W. Thiel, *Angew. Chem.* **2011**, *123*, 6996; *Angew. Chem. Int. Ed.* **2011**, *50*, 6864.
[28] G. L. Cui, Z. Lan, W. Thiel, *J. Am. Chem. Soc.* **2012**, *116*, 1510.
[29] D. Wolpert, M. Schade, T. Brixner, *J. Chem. Phys.* **2008**, *129*, 094504.
[30] D. Wolpert, M. Schade, F. Langhojer, G. Gerber, T. Brixner, *J. Phys. B* **2008**, *41*, 074025.
[31] The remaining 42 trajectories terminated because of technical problems (e.g., failure to achieve SCF convergence, energy discontinuity in two consecutive MRCI calculations, etc.) and could therefore not be used in the analysis.
[32] We note that simple photochemical processes, such as photodissociation, have been studied in small molecules by TSH simulations. See, for example: a) M. D. Lodriguito, G. Lendvay, G. C. Schatz, *J. Chem. Phys.* **2009**, *131*, 224320; b) E. Tapavicza, I. Tavernelli, U. Rothlisberger, C. Filippi, M. E. Casida, *J. Chem. Phys.* **2008**, *129*, 124108.

